Comparison of two Conservative Schemes for Hyperbolic Interface Problems

Riccardo Fazio

Dipartimento di Matematica, Università di Messina
Salita Sperone, 31, 98166 Messina, Italy
e-mail: rfazio@dipmat.unime.it

Abstract. We recall two conservative schemes recently proposed for the numerical solution of hyperbolic interface problems. Then, we compare the two schemes on a piston problem and a shock tube problem.

1 Introduction

We compare two conservative schemes for the system of conservation laws describing two gases separated by an interface. For the comparison we use a model problem introduced by Fazio and LeVeque [2]. A material interface $I(t)$ separates two gases within a tube with a piston $L(t)$ at one of its ends. The governing equations for this problem are given by Euler equations of gas dynamics,

$$\frac{\partial \mathbf{q}}{\partial t} + \frac{\partial}{\partial x}\left[\mathbf{f}(\mathbf{q})\right] = \mathbf{0} \ , \tag{1}$$

with

$$\begin{aligned} \mathbf{q} &= [\rho, \rho u, E]^T \ , \\ \mathbf{f}(\mathbf{q}) &= \left[\rho u, \rho u^2 + p, (E+p)u\right]^T \ , \end{aligned} \tag{2}$$

and with the constitutive law for ideal gases

$$p = (\gamma(x,t) - 1)\left(E - \frac{1}{2}\rho u^2\right) \ , \tag{3}$$

where ρ, u, E, and p denote, respectively, density, velocity, total energy density per unit volume, and pressure of the gas. The polytropic constant $\gamma(x,t)$ takes the value γ_1 for $0 \le x < I(t)$, and γ_2 for $I(t) < x \le L(t)$.

The motion of the piston is governed by Newton's equation

$$\frac{d^2 L}{dt^2} = \frac{A}{m}(p(L(t),t) - p_{out}(t)) \ , \tag{4}$$

where A is the area of the piston, m is its mass and $p_{out}(t)$ is a prescribed external pressure. From the above model a tube problem is recovered by assuming that the piston is initially at rest and setting $A = 0$ in (4).

2 The Eulerian scheme

For the Eulerian scheme we apply a finite volume approach, where we denote by

$$\mathbf{Q}_i^n \approx \frac{1}{\Delta x_i^n} \int_{x_i^n}^{x_i^{n+1}} \mathbf{q}(x, t_n)\, dx$$

the overage of the filed quantities on the reference grid-cell. Within the physical domain we define a moving mesh, $x_i^n < x_{i+1}^n$ at time t_n with $\Delta x_i^n = x_{i+1}^n - x_i^n$ and $\Delta t_n = t_{n+1} - t_n$. Moreover, we assume a constant speed of the moving mesh, that is

$$\dot{x}_i^n = \left(x_i^{n+1} - x_i^n\right) / \Delta t_n$$

is constant over each time step $(t_n, t_{n+1}]$.

Integrating the conservation law over the trapezoid (shown shaded in figure 1), we get

$$\Delta x_i^{n+1} \mathbf{Q}_i^{n+1} = \Delta x_i^n \mathbf{Q}_i^n - \Delta t^n \left[(\mathbf{f}(\mathbf{Q}_{i+1}^*) - \dot{x}_{i+1}^n \mathbf{Q}_{i+1}^*) - (\mathbf{f}(\mathbf{Q}_i^*) - \dot{x}_i^n \mathbf{Q}_i^*) \right] .$$

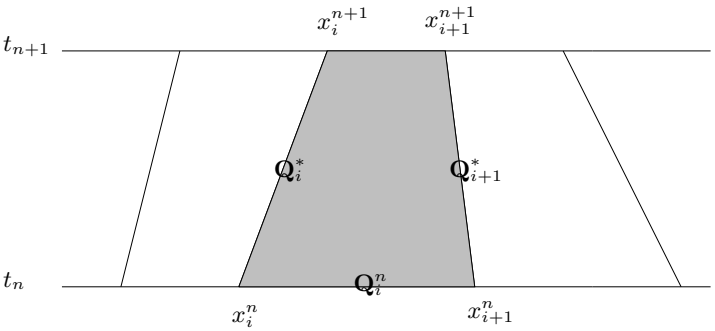

Fig. 1. Moving-mesh grid points and field quantities.

Let us define $\kappa_i^n = \Delta x_i^n / \Delta \eta$, where $\kappa(\eta, t)$ is a capacity function and η is a computational variable with constant $\Delta\eta$. Then, replacing Δx_i^n by $\kappa_i^n \Delta\eta$ in the above equation and dividing by $\Delta\eta$, we get

$$\kappa_i^{n+1} \mathbf{Q}_i^{n+1} = \kappa_i^n \mathbf{Q}_i^n - \frac{\Delta t^n}{\Delta \eta} [(\mathbf{f}(\mathbf{Q}_{i+1}^*) - \dot{x}_{i+1}^n \mathbf{Q}_{i+1}^*) - (\mathbf{f}(\mathbf{Q}_i^*) - \dot{x}_i^n \mathbf{Q}_i^*)] .$$

This gives a consistent, but nonconservative, approximation to the balance law because

$$\kappa_i^n \approx X_\eta(\eta_i, t_n) \quad \text{and} \quad \dot{x}_i^n \approx X_t(\eta_i, t_n) .$$

Note that, when the grid is moving, κ_i^n varies with n. The algorithm should achieves two goals:

1. $\sum_i \kappa_i^n Q_i^n$ should be conserved with n;
2. constant states Q should be preserved, even when κQ is varying (i.e., when the mesh is moving).

To this end, we can use the relation

$$\kappa_i^n \mathbf{Q}_i^n = \kappa_i^{n+1} \mathbf{Q}_i^n - \frac{\Delta t^n}{\Delta \eta}(\dot{x}_{i+1}^n - \dot{x}_i^n)\mathbf{Q}_i^n \ ,$$

following from $x_i^{n+1} = x_i^n + \Delta t^n \dot{x}_i^n$. The above equation, after some rearrangements, gives

$$\kappa_i^{n+1} \mathbf{Q}_i^{n+1} = \kappa_i^{n+1} \mathbf{Q}_i^n - \frac{\Delta t^n}{\Delta \eta}[(\mathbf{f}(\mathbf{Q}_{i+1}^*) - \dot{x}_{i+1}^n(\mathbf{Q}_{i+1}^* - \mathbf{Q}_i^n)) \\ -(\mathbf{f}(\mathbf{Q}_i^*) - \dot{x}_i^n(\mathbf{Q}_i^* - \mathbf{Q}_i^n))] \ .$$

This can be viewed as a conservative discretization of the balance law (see [2]).

This moving-mesh method supplemented by suitable monitor functions has been used by J. M. Stockie, J. A. Mackenzie and R. D. Russell [6] to provide a better resolution of wave structures, in particular of contact discontinuities, in comparison with fixed mesh computations.

2.1 Stability analysis

As far as the stability of the moving-mesh method is concerned, by following Harten and Hyman [4], we require that the domain of influence of the Riemann problem at x_i^n is contained in $[x_{i-1}^{n+1}, x_{i+1}^{n+1}]$ at time t^{n+1}. Hence, we impose that

$$x_{i-1}^{n+1} \le x_i^n + \lambda_i^- \Delta t^n \le x_i^n + \lambda_i^+ \Delta t^n \le x_{i+1}^{n+1} \ ,$$

where $\lambda_i^+ = max_p\,(0, \lambda_i^p)$, $\lambda_i^- = \min_p\,(0, \lambda_i^p)$, and λ_i^p is the speed of the $p-$wave, with $p = 1, 2, 3$, for the Euler equations. The above relations, by taking into account that $x_i^{n+1} = x_i^n + \Delta t^n \dot{x}_i^n$, can be unified into the stability conditions

$$|\tilde{\lambda}_i^-|\Delta t^n \le \Delta x_{i-1}^n \Rightarrow |\tilde{\lambda}_{i+1}^-|\Delta t^n \le \Delta x_i^n \\ |\tilde{\lambda}_i^+|\Delta t^n \le \Delta x_i^n \ ;$$

here $\tilde{\lambda}_i^{\pm} = \lambda_i^{\pm} - \dot{x}_i^n$ are shifted wave speeds. The two above stability restrictions can be unified into

$$\Delta t^n \max_i \left\{ \frac{\left|\tilde{\lambda}_i^+\right|}{\Delta x_i}, \frac{\left|\tilde{\lambda}_{i+1}^-\right|}{\Delta x_i} \right\} \le 1 \ . \tag{5}$$

Provided that $\dot{x}_i^n \approx \lambda_i^p$ we get wider time steps Δt^n with respect to a fixed nonuniform grid. This can be seen as a possibility to relax the global

CFL condition. However, let us note that we have three waves and only one mesh speed, so that, in general we have to find a compromise.

To grasp the reason for the shifted wave speeds in the stability condition (5), we write the transformed system

$$(\kappa(\eta,t)\,\mathbf{q})_t + [\mathbf{f}(\mathbf{q}) - \dot{x}(\eta,t)\,\mathbf{q}]_\eta = \mathbf{0}$$

in the computational variable η (here subscripts stand for partial derivatives), and notice that the new Jacobian of the flux functions is given by the old one minus the mesh speed.

A different stability condition follows by requiring Δt^n to be small enough so that waves from neighboring cells do not interact. This results in a more strict stability condition, where the left-hand side is one half than the one in (5). However, numerical tests confirm that stability is ensured by imposing (5).

3 The Lagrangian scheme

In this section, we follow the treatment by Fazio and Russo [3].

3.1 Lagrangian formulation

By introducing the Lagrangian coordinate ξ given by

$$\xi = \int_{x_0(t)}^{x} \rho(z,t)dz \ ,$$

where $x_0(t)$ denotes the Eulerian coordinate of the first fluid particle of the domain, the Euler equations (1)-(2) can be transformed in Lagrangian form

$$\frac{D\mathbf{q}}{Dt} + \frac{\partial}{\partial \xi}\left[\mathbf{f}(\mathbf{q})\right] = \mathbf{0} \ , \tag{6}$$

which is in conservation form too, with

$$\begin{aligned} \mathbf{q} &= [V, u, \mathcal{E}]^T \ , \\ \mathbf{f}(\mathbf{q}) &= [-u, p, up]^T \ ; \end{aligned} \tag{7}$$

here the time derivative is the Lagrangian derivative

$$D/Dt = \partial/\partial t + u\partial/\partial x \ ,$$

the new field variables are defined by $V(\xi,t) = \rho^{-1}, \mathcal{E} = E/\rho$, and the equation of state (3) becomes

$$p = (\gamma(\xi,t) - 1)\left(\mathcal{E} - \frac{1}{2}u^2\right)/V \ . \tag{8}$$

The inverse transformation of coordinate is

$$x = x_0(t) + \int_0^{\xi} V(z,t)dz \ , \tag{9}$$

and $x_0(t)$ satisfies the equation

$$\frac{d}{dt}x_0 = u(\xi = 0, t) \ .$$

Hence, $0 \le \xi \le \xi_{\max}$ will be our "computational domain" in which we have a fixed uniform grid with $\xi_i = (i - 1/2)\Delta\xi$, for $i = 1, 2, \ldots, N$, denoting the center of i-th cell, and $\Delta\xi = \xi_{\max}/N$.

3.2 The Nessyahu and Tadmor central scheme.

The Nessyahu and Tadmor central scheme [5] has the form of a predictor-corrector scheme

$$\mathbf{q}_j^{n+1/2} = \mathbf{q}_j^n - \frac{\lambda}{2}\mathbf{f}'_j \ ,$$
$$\mathbf{q}_{j+1/2}^{n+1} = \frac{1}{2}(\mathbf{q}_j^n + \mathbf{q}_{j+1}^n) + \frac{1}{8}(\mathbf{q}'_j - \mathbf{q}'_{j+1}) - \lambda\left(\mathbf{f}\left(\mathbf{q}_{j+1}^{n+1/2}\right) - \mathbf{f}\left(\mathbf{q}_j^{n+1/2}\right)\right) \ ,$$

where $\mathbf{q}_j^n$ denotes an approximation of the cell average of the field at time t_n

$$\mathbf{q}_j^n \approx \frac{1}{\Delta\xi}\int_{\xi_j - \Delta\xi/2}^{\xi_j + \Delta\xi/2} \mathbf{q}(\xi, t_n)\, d\xi$$

and $\lambda = \Delta t/\Delta\xi$. The time step Δt must satisfy the stability condition

$$\lambda \max_j \rho(A(\mathbf{q}_j^n)) < \frac{1}{2} \ ,$$

where $\rho(A)$ denotes the spectral radius of the Jacobian matrix

$$A = \left[\frac{\partial f_i}{\partial q_k}\right] \ .$$

This condition ensures that the generalized Riemann problems with piecewise smooth data at time t_n do not interact during the time step Δt.

$\mathbf{q}'_j/\Delta\xi$ and $\mathbf{f}'_j/\Delta\xi$ are first order approximations of the space derivatives of, respectively, the field and the flux, and can be computed in several ways. The simplest choice (used here) is

$$\mathbf{q}'_j = \mathrm{MM}(\mathbf{q}_{j+1} - \mathbf{q}_j, \mathbf{q}_j - \mathbf{q}_{j-1}) \ ,$$
$$\mathbf{f}'_j = \mathrm{MM}(\mathbf{f}_{j+1} - \mathbf{f}_j, \mathbf{f}_j - \mathbf{f}_{j-1}) \ ,$$

where $\mathrm{MM}(v, w)$ is the min-mod limiter

$$\mathrm{MM}(v, w) = \begin{cases} \mathrm{sgn}(v) \cdot \min(|v|, |w|) & \text{if } \mathrm{sgn}(v) = \mathrm{sgn}(w) \\ 0 & \text{otherwise} \ . \end{cases}$$

Let us note that, after one time step, the numerical solution is computed on a staggered grid (see Figure 2). After two time steps, the numerical solution is evaluated on the original grid.

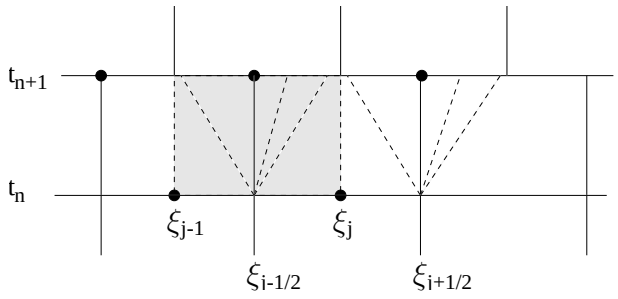

Fig. 2. Staggered grid in space-time used in the NT scheme.

3.3 Balancing the pressure at the interface.

We note that the interface is a material line and, therefore, velocity and pressure have to be continuous across the interface. This subsection report a possible way to enforce the continuity of the pressure at the interface

We assume that, at the initial time, the interface is located at the boundary between cell j_w and cell $j_w + 1$. Because of the use of Lagrangian coordinates, the interface will always separate cell j_w from cell $j_w + 1$ at even time steps, and it will be in the middle of cell $j_w + 1/2$ at odd time steps (see Figure 3).

Let us denote by subscript 1 and 2 the values of the field variables on the two sides of the interface cell at odd time steps. The balance of pressure on

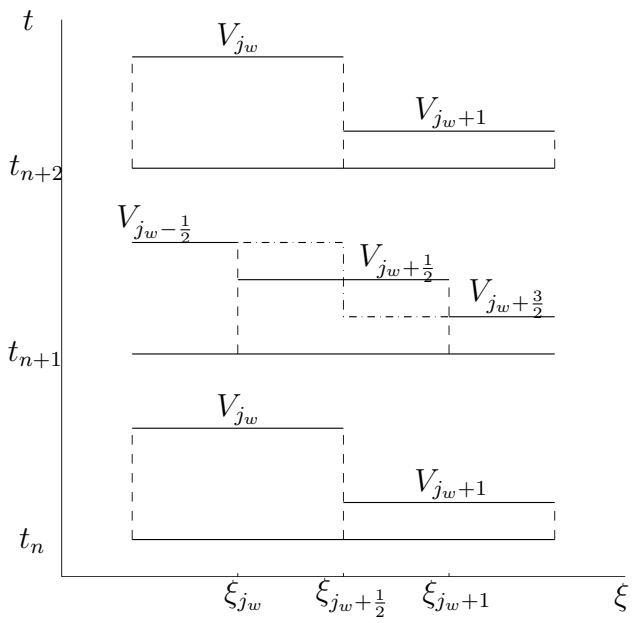

Fig. 3. Evolution of the specific volume V near the interface cell for a steady solution.

both sides of the interface, $p_1 = p_2$, gives

$$\frac{\gamma_1 - 1}{V_1}\Big(\mathcal{E}_1 - \frac{1}{2}u^2\Big) = \frac{\gamma_2 - 1}{V_2}\Big(\mathcal{E}_2 - \frac{1}{2}u^2\Big) \ . \tag{10}$$

We assume that, on the two sides of the interface, there are two different gases, whose ratio of densities, η, is equal to the ratio of molecular masses:

$$V_2 = \eta V_1 \ . \tag{11}$$

This condition is physically correct if the temperature is continuous across the interface. The cell average of specific volume V and energy $\mathcal{E}$ at the interface cell $j_w + 1/2$ are

$$V = \frac{V_1 + V_2}{2}, \quad \mathcal{E} = \frac{\mathcal{E}_1 + \mathcal{E}_2}{2} \ . \tag{12}$$

By using of above relations (10-11-12), we get the following formula for the pressure $p = p_1 = p_2$ in terms of the field variables at the interface

$$p(V, u, \mathcal{E}) = \frac{(1+\eta)(\gamma_1 - 1)(\gamma_2 - 1)}{\eta\gamma_1 + \gamma_2 - 1 - \eta}\left(\mathcal{E} - \frac{1}{2}u^2\right)/V \ . \tag{13}$$

Let us note that, by setting $\eta = 1$ and $\gamma_1 = \gamma_2 = \gamma$, we recover from (13) the classical equation of state for a polytropic gas. Once the interface quantities are known, the values of the field variables on each of the two sides can be computed

$$\begin{aligned} V_1 &= \frac{2}{1+\eta}V \ , \quad \mathcal{E}_1 = \frac{p(V,u,\mathcal{E})V_1}{\gamma_1 - 1} + \frac{1}{2}u^2 \ , \\ V_2 &= \frac{2\eta}{1+\eta}V \ , \quad \mathcal{E}_2 = \frac{p(V,u,\mathcal{E})V_2}{\gamma_2 - 1} + \frac{1}{2}u^2 \ . \end{aligned}$$

Figure 3 shows the evolution of specific volume obtained by our scheme on two time steps for a steady solution. A similar picture is obtained for the evolution of energy. Note how the scheme maintains static solutions.

4 Numerical tests

To validate the schemes we perform two tests. In particular, we consider the piston problem treated by Fazio and LeVeque [2], and the shock-interface interaction problem by Abgrall and Karni [1].

For the first test, two gases are separated by an interface between a solid wall and a plane piston. The related initial and interface conditions are

$$(\rho, u, p) = \begin{cases} (\rho_1, u_1, p_1) = (1.0, 0.0, 1.0) & 0 \le x \le I(0) \\ (\rho_2, u_2, p_2) = (1.0, 0.0, 1.0) & I(0) \le x \le L(0) \ . \end{cases}$$

$$\begin{aligned} I(0) = 0.5 \ , \quad L(0) = 1 \ , \quad \frac{dL}{dt}(0) = 0 \ , \\ \frac{dI}{dt}(t) = u_1(I(t), t) = u_2(I(t), t) \ ; \end{aligned} \tag{14}$$

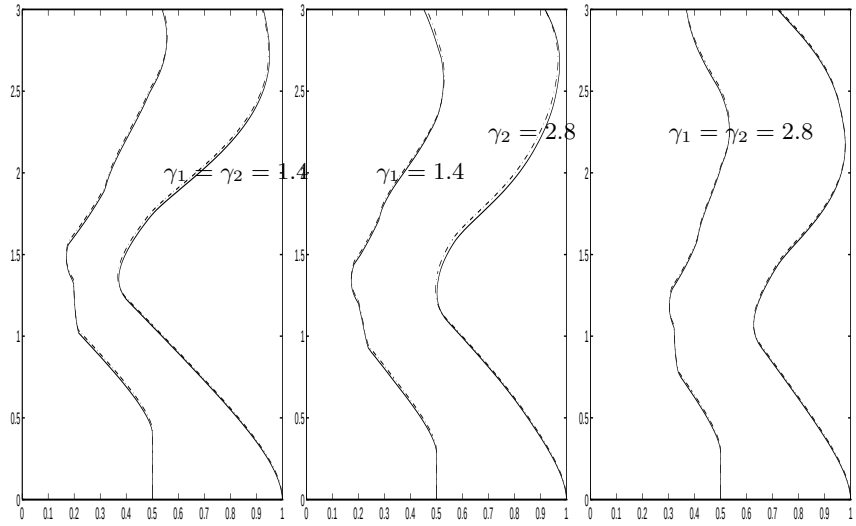

Fig. 4. Numerical results obtained with 100 mesh cells. Solid lines: Eulerian scheme implemented within CLAWPACK. Dashed-dotted lines: Lagrangian central scheme. Left $\gamma_1 = \gamma_2 = 1.4$, middle $\gamma_1 = 1.4, \gamma_2 = 2.8$ and right $\gamma_1 = \gamma_2 = 2.8$.

the remaining data are: $A/m = 2$, $p_{out}(t) = 2$, $\gamma_1 = 1.4$, $\gamma_2 = 2.8$. Figure (4) illustrates a comparison of numerical results. We plot the evolution of the interface and the piston with time, in three cases, obtained with our two different methods. The agreement of the two approaches is remarkable, considering that only 100 grid points have been used.

In the initial state the two gases are at rest, with constant pressure throughout the domain. The piston is set into motion by the (positive) difference between external and internal pressure. Let us observe that the interface does not move for a while. It starts moving when the acoustic wave, propagating inward from the piston, reaches it.

The motion of the whole system is oscillatory. The period of oscillation for the case $\gamma_1 = \gamma_2 = 1.4$ is larger than the period for the case $\gamma_1 = \gamma_2 = 2.8$, and the case of two different gases $\gamma_1 = 1.4$ and $\gamma_2 = 2.8$ is intermediate between the other two. This represents a qualitative test because the above described behaviour is the correct physical one.

The second test problem is the one proposed by Karni and Abgrall [1]. The related initial conditions are (see [1], Test case 4).

$$\begin{array}{ll} (\rho_1, u_1, p_1) = (1.0, 0.0, 500.0) & 0 \leq x < 0.5 \\ (\rho_2, u_2, p_2) = (1.0, 0.0, 0.2) & 0.5 < x \leq 1.0 \end{array} \tag{15}$$

with $\gamma_1 = 1.4$ and $\gamma_2 = 1.6$.

Figure 5 illustrates the numerical results obtained by the Eulerian scheme for the two fluid problem. In Figure 6 the calculation is repeated with the Lagrangian scheme. In both cases, we used 800 grid-points in order to permit a comparison of numerical results with the original ones obtained by Abgrall and Karni. The lack of resolution at the interface in Figure 6 is not due to

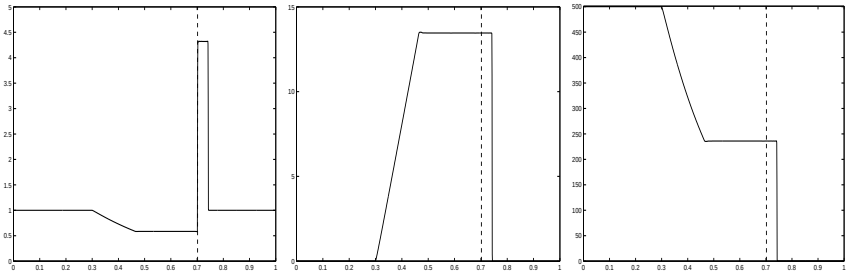

Fig. 5. Abgrall-Karni Test 4. Eulerian scheme. A dashed line indicates the position of the interface. Left: density. Center: velocity. Right: pressure.

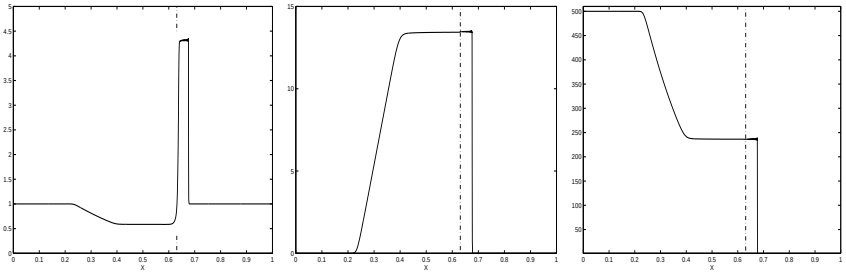

Fig. 6. Abgrall-Karni Test 4. Lagrangian scheme. A dashed line indicates the position of the interface. Left: density. Center: velocity. Right: pressure.

our treatment of the interface, but rather to the relatively poor performace of central schemes (with no artificial compression) at contact discontinuities, when compared to upwind schemes.

References

1. R. Abgrall and S. Karni. Computations of compressible multifluids. *J. Comp. Phycs.*, 169:594–623, 2001.
2. R. Fazio and R. J. LeVeque. Moving-mesh methods for one-dimensional hyperbolic problems using CLAWPACK. To appear: Comp. Math. Appl., 2003.
3. R. Fazio and G. Russo. Eulerian and Lagrangian schemes for hyperbolic interface problems. In *Eighth International Conference on Hyperbolic Problems, Teory, Numerics, Applications*, pages 121–122. Magdeburg, 28 February - 3 March, 2000. To be published.
4. A. Harten and J. M. Hyman. Self-adjusting grid methods for one-dimensional hyperbolic conservation laws. *J. Comput. Phys.*, 50:235–269, 1983.
5. H. Nessyahu and E. Tadmor. Non-oscillatory central differencing for hyperbolic conservation laws. *J. Comput. Phys.*, 87:408–463, 1990.
6. J. M. Stockie, J. A. Mackenzie, and R. D. Russell. A moving mesh method for one-dimensional hyperbolic conservation laws. *SIAM J. Sci. Comput.*, 22:1791–1813, 2001.